

Biodegradation of a PAH Mixture by Native Subsurface Microbiota

J. Steven Brauner,¹ Mark A. Widdowson,² John T. Novak,² and Nancy G. Love²

¹Parsons, 30 Dan Road, Canton, MA 02120-2809; ²200 Patton Hall, Department of Civil and Environmental Engineering, Virginia Polytechnic Institute and State University, Blacksburg, VA 24061-0105

Abstract: Laboratory microcosm studies were conducted to estimate biodegradation rates for a mixture of five polycyclic aromatic hydrocarbon compounds (PAHs). Static microcosms were assembled using soil samples from two locations collected at a No. 2 fuel oil-contaminated site in the Atlantic Coastal Plain of Virginia. In microcosms from one location, five PAHs (acenaphthene, fluorene, phenanthrene, pyrene, and benzo(b)fluoranthene) biodegraded at net first-order rates of 1.08, 1.45, 1.13, 1.11, and 1.12 yr⁻¹, respectively. No observable lag period was noted and degradation in live microcosms ceased with the depletion of oxygen and sulfate after 125 days. In microcosms from a second location, net first-order biodegradation rates after an approximately 2-month lag period were 2.41, 3.28, and 2.98 yr⁻¹ for fluorene, phenanthrene, and pyrene, respectively. Acenaphthene and benzo(b)fluoranthene mass loss rates in the live microcosms were not statistically different from mass loss rates in control microcosms. Stoichiometric mass balance calculations indicate that the dominant PAH mass loss mechanism was aerobic biodegradation, while abiotic losses (attributed to micropore diffusion and oxidative coupling) ranged from 15 to 33% and biotic losses from sulfate-reduction accounted for 7 to 10% of PAH mass loss. Stoichiometric equations that include biomass yield are presented for PAH oxidation under aerobic and sulfate-reducing conditions.

Key Words: PAH, biodegradation, natural attenuation, microcosm, sulfate-reduction.

Introduction

Polycyclic aromatic hydrocarbon compounds (PAHs) are a class of compounds derived from complex non-aqueous phase liquids, specifically coal tars, creosote and various fuels, that are listed as United States Environmental Protection Agency (USEPA) priority pollutants (Peters *et al.*, 1999). PAHs are characterized by two or more joined benzene rings and exhibit a wide range of physical and chemical properties (e.g., solubility and molecular weight). The mobility of PAHs in soil and groundwater decreases with increasing molecular weight (Peters *et al.*, 1999). Low-molecular-weight PAH compounds have been shown to biodegrade under certain environmental conditions, while higher-molecular-weight PAH compounds are

relatively recalcitrant (Brown *et al.*, 1999). The recent report of the National Research Council (NRC) lists the likelihood of success of monitored natural attenuation (MNA) for PAHs as "low", given the current level of understanding (NRC, 2000).

Previous research has demonstrated PAH biodegradation under oxic conditions when an appropriate mixture of microorganisms, nutrients, and oxygen were present (e.g., Bauer and Capone, 1988; Gibson *et al.*, 1975; Leduc *et al.*, 1992). Biotransformation of acenaphthene, acenaphthylene, anthracene, fluorene, naphthalene, and phenanthrene, and pyrene under strictly anaerobic, nitrate-reducing conditions has also been shown to occur (Leduc *et al.*, 1992; McNally *et al.*, 1998; Mihelcic and Luthy, 1988a; b). Two recent studies demonstrated PAH biodegradation under sul-

fate-reducing conditions, in which a native microbial population collected with marine sediments was shown to biodegrade fluorene, fluoranthene, naphthalene, and phenanthrene (Coates *et al.*, 1996, 1997). Another study found that the size and PAH biodegradation capabilities of a native freshwater microbial population varied with location in samples collected from a former manufactured gas plant site (Durant *et al.*, 1995). Although previous studies have demonstrated that many PAH compounds will biodegrade under at least oxic conditions, the extent of PAH biodegradation by native microbial consortia is not fully known when these compounds are found as a mixed substrate. For example, Juhasz *et al.* (2000) reported that fluorene and naphthalene were degraded to a larger extent relative to three- and four-ring PAH compounds by an indigenous microflora in laboratory-incubated soil samples collected at a petrochemical site.

For recalcitrant compounds such as PAHs, regulatory acceptance of MNA as a remediation strategy requires site-specific data to demonstrate attenuation of contaminants that are of health and environmental concern (NRC, 2000). One line of evidence for determining the feasibility of MNA as part of a corrective action plan is to perform microcosm experiments using soil samples collected from that site to demonstrate contaminant biodegradation under simulated natural conditions (USEPA, 1999). Furthermore, the ability of a native microbial consortium to biodegrade PAH mixtures can be determined, and the effectiveness of microbial transformations to attenuate contaminants at PAH sites under intrinsic conditions can be assessed.

The goal of this study was to establish (1) whether a native, nonspecific microbial consortia, collected with soil samples at a heating fuel-contaminated site, was able to biologically transform a mixture of five PAH compounds under simulated intrinsic conditions, and (2) to determine the degradation rates for the individual PAHs in two soils with different contamination histories. The term “intrinsic conditions” is intended to refer to field conditions or laboratory experiments in which biostimulation (i.e., addition of electron acceptors, nutrients, and cometabolites) and/or bioaugmentation (i.e., addition of specific cultures of microorganisms) was not employed to stimulate PAH biodegradation.

Soil samples were collected from two locations at the site, and differences in PAH biodegradation were observed as a function of both the PAH compound and the sample location. The PAHs investigated in this study (acenaphthene, benzo(*b*)fluoranthene, fluorene, phenanthrene, and pyrene) were selected based on a previous site investigation completed immediately prior to this study that demonstrated PAH compounds were

present in soil and groundwater at numerous sampling locations and at levels that required corrective action (Lee, personal communication). Biodegradation rates for PAHs were estimated using the difference in mass loss rates between live and control (autoclaved) microcosms. The relative contribution of aerobic and sulfate-reducing microorganisms to the overall reduction in PAH concentration was determined by calculating the theoretical mass of PAH that could be biodegraded for the observed mass of electron acceptor consumed. Two stoichiometric methods for calculating theoretical PAH mass loss were applied and compared with the observed PAH mass loss.

Methods

Site Selection and Soil Collection

Soil samples were collected from two locations at a petroleum-contaminated site in the Atlantic Coastal Plain of Fairfax County, Virginia. No. 2 fuel oil had leaked from multiple, small underground storage tanks (USTs) and underground fuel supply lines serving residential housing. One soil sample (hereafter referred to as Sample A) was collected from well cuttings brought to the surface during the installation of a monitoring well. Sample A consisted of orange-brown, clayey sand, and was collected from an area previously shown to be highly contaminated with fuel oil. Table 1 shows the range of acenaphthene, fluorene, phenanthrene, and pyrene concentrations that were measured in this area. A second soil sample (hereafter referred to as Sample B) consisted of a yellow-brown, sandy clay that was collected approximately 2 ft below land surface using a hand auger. Sample B was collected near a location where a leaking UST had been excavated recently. Analysis of Sample B using mass chromatographic mass spectrometry (GC-MS) detected some alkanes, but no PAHs. Both samples were collected aseptically, placed in sterilized jars, and transported to the laboratory where they were stored at 20°C until used in the microcosm experiment.

Microcosm Construction

A live and control microcosm batch was constructed for each soil sample, resulting in a total of four microcosm batches (Sample A live, Sample B live, Sample A control, and Sample B control). Contents for each microcosm batch were prepared under aerobic conditions and placed in sterilized, 10 mL, threaded test tubes that were then sealed with Teflon®-lined caps. Sample A and Sample B soil samples were homogenized by breaking soil particles that were more than a few millimeters in diameter into smaller pieces using a mortar and pestle. This homogenization procedure

Table 1. PAH concentrations measured in the vicinity of the collection location for Sample A

Compound	Minimum Field Concentration [$\mu\text{g}/\text{kg}$]	Maximum Field Concentration [$\mu\text{g}/\text{kg}$]
Acenaphthene	480	5,300
Fluorene	220	14,000
Phenanthrene	BD	90,000
Pyrene	BD	77

was performed to allow a more uniform distribution of PAHs during PAH addition (described below) and to facilitate the addition of soil to the microcosm test tubes. The total masses of Sample A and Sample B following the homogenization procedure were 932 g and 2029 g, respectively. Approximately 85% of each sample (809 g of Sample A and 1719 g of Sample B) was allocated for use in live microcosms, while the remaining 15% was (123 g of Sample A and 300 g of Sample B) was allocated for abiotic control microcosms. The procedure for constructing both live and control microcosms was identical except that the soil for the control microcosms was repeatedly autoclaved (10 repetitions of 25-min duration at 121°C and 15 psi), while the live soil was not. Approximately 40% of each microcosm batch soil (309 g of Sample A live, 716 g of Sample B live, 50 g of Sample A control, and 121 g of Sample B control) was treated with a mixture of PAHs (equal masses of acenaphthene, fluorene, phenanthrene, pyrene, and benzo(*b*)fluoranthene) dissolved in hexane. All five PAHs were laboratory grade and obtained from Supelco. The goal of the PAH addition was to increase the concentration of these selected PAHs to a level that was closer to the maximum concentrations measured in the field and reported in Table 1. The PAH/hexane/soil mixture was then rotated for 4 h to promote thorough mixing between the PAH and soil. Following this mixing procedure, the solvent (hexane) was allowed to evaporate from each sample. The remaining 40% of each soil batch (500 g of Sample A live, 1013 g of Sample B live, 73 g of Sample A control, and 179 g of Sample B control), which had not been contacted with hexane to preserve the native microbiota, was then mixed with the corresponding portion of freshly PAH-contaminated soil. A small portion (~ 5 g) of the mixed soil was added to each microcosm along with 5 mL of deionized, autoclaved water. Other than providing a fresh source of PAHs and oxygen (in the deionized

water), no other chemical or biological amendments were added to the microcosms. The microcosms were incubated statically in the dark at 12°C until sacrificed in triplicate using the analytical procedure discussed below.

Analytical Methods

PAH compounds were extracted from each microcosm by combining the microcosm contents with 15 mL of methylene chloride (CH_2Cl_2) in 40-mL amber vials. The 40-mL vials were sealed with screw-on caps containing Teflon[®] coated septa and rotated for 24 h to promote thorough contact between the microcosm contents and CH_2Cl_2 . After rotation, the contents of the 40-mL vials were allowed to settle and were stored in the dark at 4°C for a minimum of 4 h and maximum of 24 h prior to analysis by a gas chromatograph using an HP-5890 gas chromatograph with a flame ionization detector (GC-FID) and a J&W Scientific DB-5 ms capillary column. The GC-FID temperature program consisted of an initial temperature hold of 1 min at 65°C, followed by a temperature increase to 300°C at a rate of 10°C per minute and a final hold of 9 min at 300°C. Extractable PAHs were measured in duplicate by injecting a 2- μL sample into the GC-FID. PAH concentrations (mg PAH per liter CH_2Cl_2) were quantified using a series of external standards (Supelco) and converted to mass of PAH per mass of soil by considering the volume of solvent (15 mL) and initial mass of soil (5 g) in each microcosm vial.

Dissolved oxygen (DO) was measured using a Diamond Electric Microsensor II connected to a PO_2 Needle Electrode. A two-point calibration procedure was performed by successively bubbling nitrogen gas (0% oxygen) and breathing air (21% oxygen) through a calibration cell. Electrode calibration was monitored and adjusted (when needed) before and after each set of measurements to account for the effects of drift inherent to the probe. Nitrate and sulfate concentra-

tions were measured concurrently by removing approximately 1.5 mL of water from the microcosms (prior to CH₂Cl₂ extraction) and analyzing the sample using ion chromatography (IC) according to method 4110B in Standard Methods (APHA, 1998). Prior to injection into the ion chromatograph, the sample was filtered using an IC syringe filter (0.45 μm pore size, polyethersulfone, hydrophilic, bidirectional membrane). External standards were used to calculate nitrate and sulfate concentrations.

Degradation Rate Estimation

PAH degradation rates were calculated using a linear regression on log transformed PAH concentrations, yielding first-order exponential rate constants. PAH degradation rates in the control microcosms were calculated using all available data points. PAH degradation rates in the live microcosms were calculated from the end of any observed period of acclimation to any point where the rate of degradation matched the rate of degradation of the control microcosms. This latter point typically coincided with depletion of oxygen in the live microcosms.

Statistical comparison of degradation rates in the live and control microcosms was accomplished using a method similar to that developed in a previous microcosm study on slowly degrading chlorinated compounds (Wilson *et al.*, 1996). The degradation rate in the live microcosms was considered statistically greater than the rate in the control microcosms when the 95% confidence interval of the degradation rate in the live microcosms did not include the average degradation rate of the controls. Net degradation rates were calculated as the difference between the degradation rates in the live and control microcosms. Confidence intervals for the net degradation rates of each compound were developed using a previously described regression analysis technique for statistically determining the difference in slope (Ott, 1992).

Stoichiometric Mass Balance Procedure

Stoichiometric mass balance equations were developed to estimate the mass of PAH that could theoretically be oxidized to carbon dioxide (e.g., Coates *et al.*, 1996) for observed changes in electron acceptor mass. Because the five PAHs added during microcosm construction served as a mixed substrate, calculations for the theoretical PAH mass loss was estimated as the total for all five PAHs. A theoretical estimate for the total PAH mass mineralized under electron accepting condition n ($\Delta\text{PAH}_n^{\text{theoretical}}$) was estimated using

$$\Delta\text{PAH}_n^{\text{theoretical}} = \frac{\Delta EA_n^{\text{observed}}}{\bar{\gamma}_n} \quad (1)$$

where $\Delta EA_n^{\text{observed}}$ was the observed mass of electron acceptor n consumed and $\bar{\gamma}_n$ was the mean electron acceptor use coefficient for the mass of electron acceptor n reduced per mass of PAH mineralized [M_{EA}/M_{PAH}]. The aqueous phase $\Delta EA_n^{\text{observed}}$ was estimated by subtracting the difference between the electron acceptor concentration measured in the live microcosms at the end of the experiment from the concentrations measured in the controls and multiplying this concentration differential by the volume of water in the microcosm (5 mL).

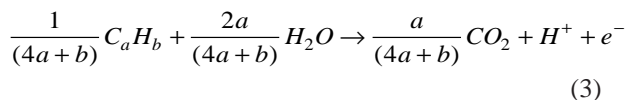
The mass of oxygen in the headspace was included in the total mass of consumed electron acceptor. Gaseous oxygen was assumed to readily diffuse from the headspace into the aqueous phase to replenish aqueous phase oxygen consumed during biodegradation. The gaseous phase contribution of oxygen to $\Delta EA_n^{\text{observed}}$ was calculated by assuming 21% oxygen in the 2.5-mL headspace at time zero and that the microcosms were tightly sealed, preventing the escape or addition of oxygen over time.

For the PAH mixture used in this experiment ($K = 5$), $\bar{\gamma}_n$ was estimated as

$$\bar{\gamma}_n = \frac{1}{K} \sum_{k=1}^{K=5} \gamma_{k,n} \quad (2)$$

where $\gamma_{k,n}$ was the use coefficient for mineralization of PAH k under electron acceptor condition n . Each electron acceptor use coefficient was calculated based on PAH and electron acceptor molecular weights and the molar ratio of PAH to electron acceptor estimated from stoichiometrically balanced equations. The molar ratios were developed using half-cell reactions for PAH mineralization and electron acceptor reduction. The least complex stoichiometric formulation assumes that the PAHs were the sole electron donors, carbon dioxide and water were the only products, and none of the hydrocarbon was converted to biomass (i.e., zero yield). Half-cell reactions for phenanthrene and pyrene mineralization (McFarland and Sims, 1991) and electron acceptor reduction (Zehnder and Stumm, 1988) have been developed previously, whereas half-cell reactions for acenaphthene, fluorene, and benzo(*b*)fluoranthene

mineralization were developed in this study using the general electron donor half cell reaction given by



and described in (Stumm and Morgan, 1995). The constants a and b in Equation 3 represent the number of carbon and hydrogen atoms, respectively, in the original hydrocarbon compound.

Table 2 contains the stoichiometric equations for the zero yield case for all five PAHs under aerobic and sulfate-reducing conditions. Table 3 contains electron acceptor use coefficients for each PAH under aerobic and sulfate-reducing conditions for the zero yield case, which were calculated using the stoichiometric ratios from Table 2. As shown in Table 3, this zero-yield method resulted in an $\bar{\gamma}_n$ estimate of 2.96 mg_{O2}/mg_{PAH} and 4.45 mg_{SO4}/mg_{PAH} for aerobic and sulfate-reducing conditions, respectively.

Because the stoichiometric formulations in Table 2 neglect biomass yield, the values for $\bar{\gamma}_n$ presented in Table 3 may result in an underestimation of the theoretical mass of PAH mineralized for a given mass of electron acceptor consumed. Grady *et al.* (1999) demonstrated that stoichiometric formulations could account for microbial growth by assuming that a portion of the carbon growth substrate was converted to biomass and treating biomass production as a reaction end product given by the empirical formula C₅H₇O₂N. This method also incorporated a biomass yield coefficient (Y) to account for the efficiency of biomass produc-

tion on a given growth substrate (Grady *et al.*, 1999). Theoretical estimates for the average biomass yield during PAH oxidation under aerobic and sulfate-reducing conditions have been reported as 0.33 g_{biomass}/g_{PAH} and 0.06 g_{biomass}/g_{PAH}, respectively (McFarland and Sims, 1991), using a bioenergetic model that assumed ammonium was a nonlimiting source of nitrogen (McCarty, 1971).

For the present study, stoichiometric equations developed for PAH oxidation to CO₂ under aerobic and sulfate-reducing conditions that include biomass yield are given in Table 4. These relationships are based on theoretical estimates for yield coefficients under aerobic and sulfate-reducing conditions given in McFarland and Sims (1991). Electron acceptor use coefficients for each PAH are presented in Table 5. Values for $\bar{\gamma}_n$ are estimated as 1.98 mg_{O2}/mg_{PAH} and 4.18 mg_{SO4}/mg_{PAH} for aerobic and sulfate-reducing conditions, respectively, when yield was included in the stoichiometric equations.

Results and Discussion

PAH Degradation and Electron Acceptor Mass Loss

Sample A. Results for PAH concentration versus time are reported in Figure 1 for each of the five PAH compounds measured in the Sample A live and control microcosms. Each data point represents the average concentration of three sacrificially sampled microcosms, with error bars representing \pm one standard deviation. The starting concentrations of the five PAHs

Table 2. Oxidation-reduction reactions for PAH mineralization to carbon dioxide under aerobic and sulfate-reducing conditions, assuming zero biomass yield

Compound	Stoichiometric Mass Balance Equation
Acenaphthene	$C_{12}H_{10} + 14.5 O_2 \rightarrow 12 CO_2 + 5 H_2O$
	$C_{12}H_{10} + 7.25 SO_4^{2-} + 10.88 H^+ \rightarrow 12 CO_2 + 3.63 H_2S + 3.63 HS^- + 5 H_2O$
Fluorene	$C_{13}H_{10} + 15.5 O_2 \rightarrow 13 CO_2 + 5 H_2O$
	$C_{13}H_{10} + 7.75 SO_4^{2-} + 11.63 H^+ \rightarrow 13 CO_2 + 3.88 H_2S + 3.88 HS^- + 5 H_2O$
Phenanthrene	$C_{14}H_{10} + 16.5 O_2 \rightarrow 14 CO_2 + 5 H_2O$
	$C_{14}H_{10} + 8.25 SO_4^{2-} + 12.38 H^+ \rightarrow 14 CO_2 + 4.13 H_2S + 4.13 HS^- + 5 H_2O$
Pyrene	$C_{16}H_{10} + 18.5 O_2 \rightarrow 16 CO_2 + 5 H_2O$
	$C_{16}H_{10} + 9.25 SO_4^{2-} + 13.88 H^+ \rightarrow 16 CO_2 + 4.63 H_2S + 4.63 HS^- + 5 H_2O$
Benzo(b)fluoranthene	$C_{20}H_{12} + 23 O_2 \rightarrow 20 CO_2 + 6 H_2O$
	$C_{20}H_{12} + 11.5 SO_4^{2-} + 17.25 H^+ \rightarrow 20 CO_2 + 5.75 H_2S + 5.75 HS^- + 6 H_2O$

Table 3. Electron acceptor use coefficients by PAH and electron acceptor condition for stoichiometric calculations assuming zero biomass yield

Compound	Use Coefficient, $\gamma_{m,n}$	
	Aerobic [mgO ₂ /mgPAH]	Sulfate-Reducing [mgSO ₄ /mgPAH]
Acenaphthene	3.01	4.52
Fluorene	2.98	4.48
Phenanthrene	2.96	4.45
Pyrene	2.93	4.39
Benzo(b)fluoranthene	2.92	4.39
Average ($\bar{\gamma}_n$) =	2.96	4.45

Table 4. Oxidation-reduction reactions for PAH mineralization to carbon dioxide under aerobic and sulfate-reducing conditions, assuming biomass yield and a non-limiting mass of reduced nitrogen. Yield coefficients (mg biomass/mg PAH) for the aerobic and sulfate-reducing microbial populations were assumed equal to 0.33 and 0.06, respectively

Compound	Stoichiometric Mass Balance Equation
Acenaphthene	$C_{12}H_{10} + 9.7 O_2 + 0.96 HCO_3^- + 0.96 NH_4^+ \rightarrow 8.2 CO_2 + 0.96 C_5H_7O_2N + 4.0 H_2O$ $C_{12}H_{10} + 6.8 SO_4^{2-} + 10.2 H^+ + 0.17 HCO_3^- + 0.17 NH_4^+ \rightarrow$ $11.3 CO_2 + 0.17 C_5H_7O_2N + 3.4 H_2S + 3.4 HS^- + 4.8 H_2O$
Fluorene	$C_{13}H_{10} + 10.4 O_2 + 1.02 HCO_3^- + 1.02 NH_4^+ \rightarrow 8.9 CO_2 + 1.02 C_5H_7O_2N + 4.0 H_2O$ $C_{13}H_{10} + 7.3 SO_4^{2-} + 10.9 H^+ + 0.19 HCO_3^- + 0.19 NH_4^+ \rightarrow$ $12.3 CO_2 + 0.19 C_5H_7O_2N + 3.6 H_2S + 3.6 HS^- + 4.8 H_2O$
Phenanthrene	$C_{14}H_{10} + 11.1 O_2 + 1.09 HCO_3^- + 1.09 NH_4^+ \rightarrow 9.6 CO_2 + 1.09 C_5H_7O_2N + 3.9 H_2O$ $C_{14}H_{10} + 7.8 SO_4^{2-} + 11.6 H^+ + 0.20 HCO_3^- + 0.20 NH_4^+ \rightarrow$ $13.2 CO_2 + 0.20 C_5H_7O_2N + 3.9 H_2S + 3.9 HS^- + 4.8 H_2O$
Pyrene	$C_{16}H_{10} + 12.4 O_2 + 1.22 HCO_3^- + 1.22 NH_4^+ \rightarrow 11.1 CO_2 + 1.22 C_5H_7O_2N + 3.8 H_2O$ $C_{16}H_{10} + 8.7 SO_4^{2-} + 13.0 H^+ + 0.22 HCO_3^- + 0.22 NH_4^+ \rightarrow$ $15.1 CO_2 + 0.22 C_5H_7O_2N + 4.3 H_2S + 4.3 HS^- + 4.8 H_2O$
Benzo(b)fluoranthene	$C_{20}H_{12} + 15.4 O_2 + 1.52 HCO_3^- + 1.52 NH_4^+ \rightarrow 13.9 CO_2 + 1.52 C_5H_7O_2N + 5 H_2O$ $C_{20}H_{12} + 10.8 SO_4^{2-} + 16.2 H^+ + 0.28 HCO_3^- + 0.28 NH_4^+ \rightarrow$ $18.9 CO_2 + 0.28 C_5H_7O_2N + 5.4 H_2S + 5.4 HS^- + 5.7 H_2O$

Table 5. Electron acceptor use for stoichiometric calculations when yield coefficients (mg biomass/mg PAH) of 0.33 and 0.06 were used for the aerobic and sulfate-reducing microbial populations, respectively

Compound	Use Coefficient, $\gamma_{m,n}$	
	Aerobic [mg _{O2} /mg _{PAH}]	Sulfate-Reducing [mg _{SO4} /mg _{PAH}]
Acenaphthene	2.02	4.25
Fluorene	2.00	4.21
Phenanthrene	1.98	4.18
Pyrene	1.96	4.13
Benzo(b)fluoranthene	1.96	4.12
Average ($\bar{\gamma}_n$) =	1.98	4.18

ranged between 15 and 100 mg_{PAH}/kg_{soil} and were consistent with the range of maximum PAH concentrations measured at the site. The slopes of the best fit lines through the first nine data points in the Sample A live microcosms and all of the data points in the Sample A control microcosms are reported in Table 6 as the live and control degradation rates, respectively, for each PAH.

During the first 112 to 125 days of the experiment, PAH mass loss rates in the Sample A live microcosms ranged from 1.38 year⁻¹ to 1.91 year⁻¹. The PAH degradation rates for the live microcosms were greater than the rates observed for the Sample A controls, which ranged from 0.27 to 0.63 year⁻¹. Statistical regression ($p \leq 0.05$) of Sample A degradation rates, calculated using log-transformed data, showed that rates of removal were statistically greater in the live microcosms than in the control microcosms for all five PAHs. The net first-order degradation rates, calculated as the difference between the degradation rate in the live and control microcosms, are listed for Sample A in Table 6. After approximately 112 to 125 days into the experiment, mass loss rates in the Sample A live microcosms (computed from the last four data points) were statistically similar to mass loss rates in the control microcosms for all five PAHs. R-squared values for Sample A controls varied over a wider range (0.43 to 0.88) than values for the Sample A live samples during the initial degradation period (0.75 to 0.90).

Dissolved oxygen concentrations measured at Day 112 were below detection (less than 0.1 mg/L) in the Sample A live microcosms, indicating that the available oxygen had been consumed. In the Sample A control microcosms, the concentration of dissolved oxygen was 3.4 (\pm 0.2) mg/L at Day 218. Sulfate

concentrations in the live microcosms were 1.2 (\pm 0.9) mg/L at Day 218. In comparison, sulfate concentration in the Sample A control microcosms was 53 (\pm 2.3) mg/L at Day 218. Concentrations of nitrate in both live and control microcosms were less than 1 mg/L for all samples tested and had not varied from the initial concentration of nitrate. This result indicates that microbially mediated nitrate consumption was minimal and that little or no PAH oxidation occurred due to nitrate reduction.

Sample B. Results for PAH concentration vs. time are reported in Figure 2 for acenaphthene, fluorene, phenanthrene and pyrene in the Sample B live and control microcosms. Statistical analysis comparing the degradation rates for acenaphthene and benzo(b)fluoranthene (data not shown) in the live microcosms with rates calculated from the control microcosms indicated that there was no difference in slope between live and controls for these two compounds. For fluorene, phenanthrene, and pyrene, statistical analysis comparing the slopes of the best fit lines through the data points 5 through 9 of the Sample B live microcosms and all of the data points in the Sample B control microcosms showed that the degradation rate of these three compounds in the live microcosms was greater than that calculated from the controls. The Sample B net degradation rates for all five PAHs are reported in Table 7. R-squared values for Sample B controls varied over a wider range (0.44 to 0.86) than values for the Sample B live samples during the second degradation period (0.74 to 0.99).

Dissolved oxygen concentrations recorded 119 days into the experiment were below detection (less than 0.1 mg/L) in the Sample B live microcosms, indicating that the available oxygen had been con-

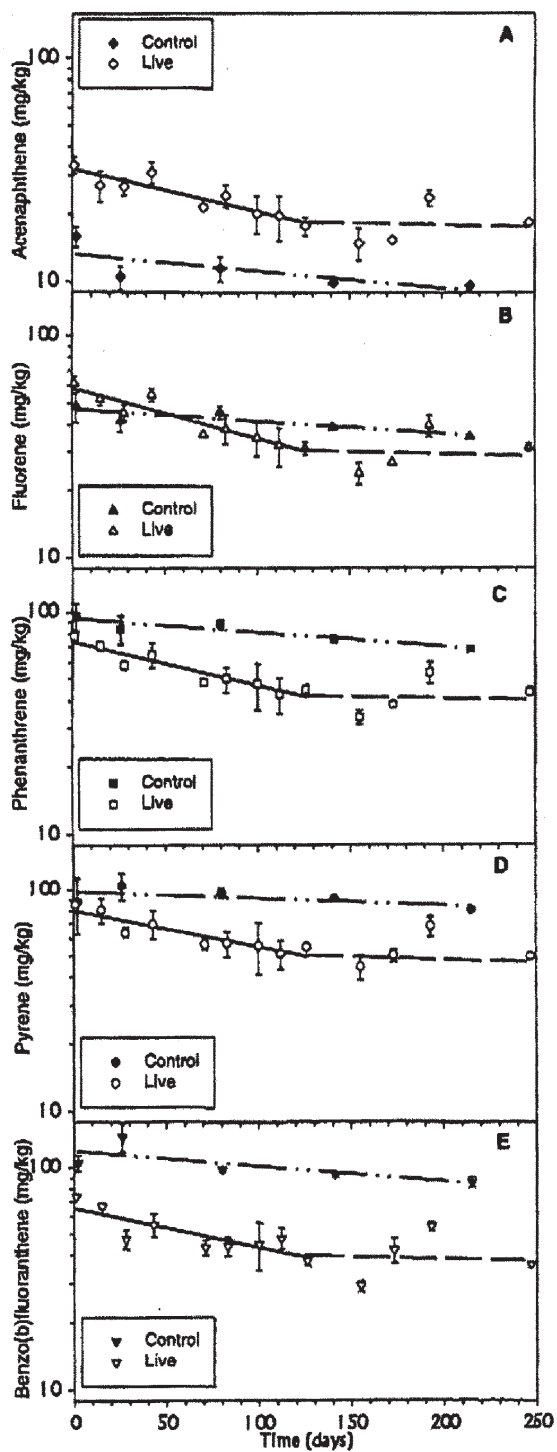


Figure 1. Concentration vs. time for (A) acenaphthene, (B) fluorene, (C) phenanthrene, (D) pyrene, and (E) benzo(b)fluoranthene in microcosms containing soil from Sample A. The dash dotted (— · —) line represents the best fit regression line for the control microcosms. The solid (—) line represents the best fit through the live microcosms during the 'active' phase, while the dashed (— —) line represents the best fit line during periods when the live microcosms were inactive. Error bars represent \pm one standard deviation in the concentration measurement.

Table 6. First-order rate constants, confidence intervals, and R-squared coefficients for disappearance of selected PAH compounds in microcosms containing soil from Sample A

Compound	Live Microcosms			Control Microcosms			Net		
	Degradation Rate [year ⁻¹]	(± 95% C.I.) [year ⁻¹]	R ²	Degradation Rate [year ⁻¹]	(± 95% C.I.) [year ⁻¹]	R ²	Degradation Rate [year ⁻¹]	(± 95% C.I.) [year ⁻¹]	R ²
Acenaphthene	-1.71	(±0.48)	0.87	-0.63	(±1.06)	0.55	-1.08	(±0.78)	0.55
Fluorene	-1.91	(±0.60)	0.89	-0.46	(±0.47)	0.77	-1.45	(±0.66)	0.77
Phenanthrene	-1.65	(±0.50)	0.90	-0.52	(±0.36)	0.88	-1.13	(±0.54)	0.88
Pyrene	-1.38	(±0.53)	0.84	-0.27	(±0.57)	0.43	-1.11	(±0.64)	0.43
Benzo(b)fluoranthene	-1.71	(±0.68)	0.75	-0.58	(±0.92)	0.58	-1.12	(±0.89)	0.58

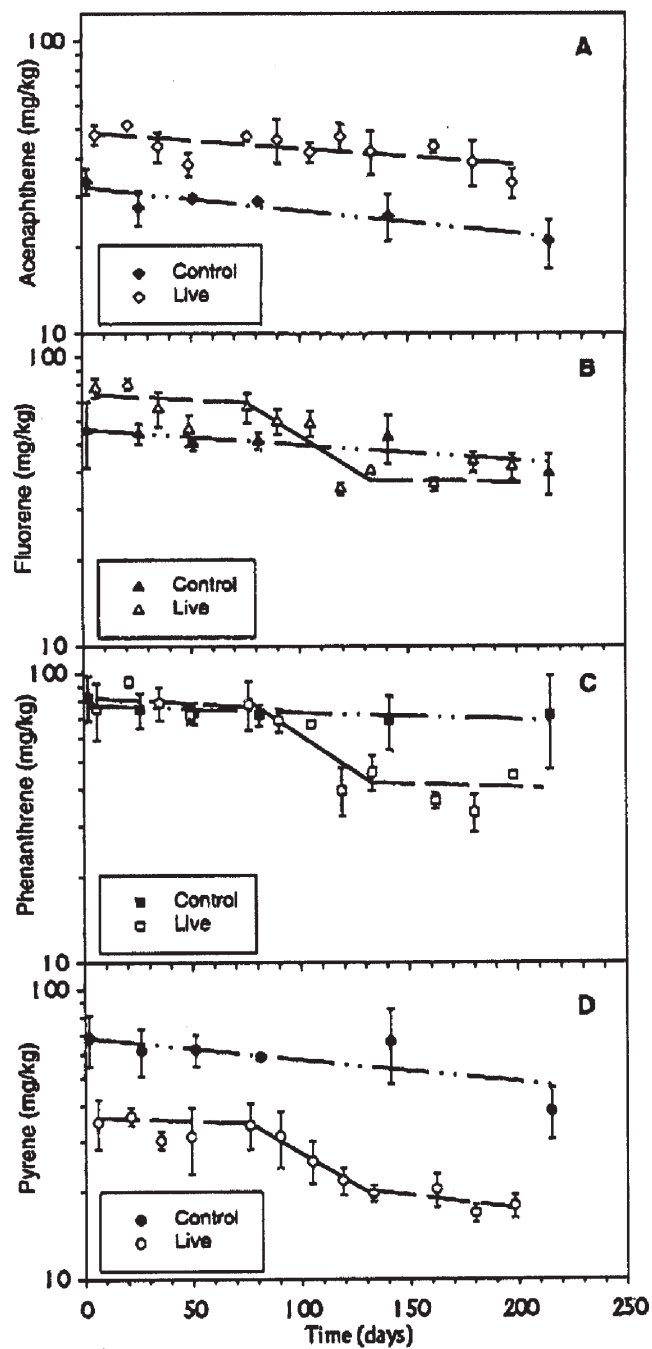


Figure 2. PAH concentration versus time for (A) acenaphthene, (B) fluorene, (C) phenanthrene, and (D) pyrene in microcosms containing soil from Sample B. The dash dotted (— · —) line represents the best fit regression line for the control microcosms. The solid (—) line represents the best fit through the live microcosms during the 'active' phase, while the dashed (— —) line represents the best fit line during periods when the live microcosms were inactive. Error bars represent \pm one standard deviation in the concentration measurement. (Modified from Brauner *et al.*, 1999.)

Table 7. Comparison of net degradation rate constants in the Sample A and Sample B microcosms

Compound	Degradation Rate	
	Sample A [year ⁻¹]	Sample B ^a [year ⁻¹]
Acenaphthene	-1.08	0.0 ^b
Fluorene	-1.45	-2.41
Phenanthrene	-1.13	-3.28
Pyrene	-1.11	-2.98
Benzo(b)fluoranthene	-1.12	0.0 ^b

^a First-order degradation rates for a soil sample collected from a location of the site where PAH compounds were not found, as reported previously (Brauner *et al.*, 1999).

^b Biodegradation of acenaphthene and benzo(b)fluoranthene was not observed in the PAH degradation microcosm study conducted using soil from Sample B.

sumed. Dissolved oxygen concentrations in the Sample B control microcosms were 4.8 (\pm 0.7) mg/L at Day 227. Sulfate concentrations in the Sample B live microcosms were 11.5 (\pm 0.9) mg/L at Day 227, which was less than the sulfate concentration of 34.4 (\pm 1.8) mg/L measured in the Sample B control microcosms at Day 227. Although sulfate in the Sample B live microcosms was not fully depleted, the reduction in sulfate concentration relative to the Sample B control microcosms suggests that microbially-mediated sulfate utilization occurred in the Sample B live microcosms. As with the Sample A microcosms, measured concentrations of nitrate were less than 1 mg/L for all samples tested and had not varied from the initial concentration of nitrate. The absence of nitrate suggests that little or no PAH oxidation occurred due to nitrate reduction. **Controls.** Irreversible abiotic processes produced by a combination of micropore diffusion, oxidative coupling, and volatilization were thought to be responsible for PAH mass losses in the control microcosms. Several studies have shown that long contact times between PAHs and soil may result in a decrease in extractable hydrocarbon mass with time (Hatzinger and Alexander, 1995; Karickhoff, 1980). These researchers attributed this phenomenon to diffusion of hydrophobic compounds into soil micropores when contact times were on the order of several days to several months. Additional research has suggested that oxidative coupling can irreversibly bind PAH compounds and their intermediates to soil (Novak *et al.*, 1998), further contributing to abiotic losses observed during microcosm studies. The solvent extraction pro-

cedure used in this study only measured the combined mass of aqueous and ‘reversibly’ sorbed PAH per dry soil mass because the portion of irreversibly sorbed or bound PAH mass was not likely to be extracted into the CH₂Cl₂.

Estimated Biodegradation Rates. Based on the statistically greater mass loss rates calculated for all PAHs in the Sample A live microcosms and for fluorene, phenanthrene, and pyrene in the Sample B live microcosms, relative to their respective control microcosms, it was evident that biodegradation was responsible for a portion of PAH mass loss in the live microcosms. The observed depletion of oxygen and decline in sulfate concentrations coincided with PAH disappearance in the live microcosms, suggesting that aerobic and sulfate-reducing microorganisms were active during PAH biodegradation in the Sample A microcosms. It is not known whether all PAH compounds were biodegraded as a result of both terminal electron accepting processes. PAH biodegradation in the Sample A microcosms was believed to have ceased between Day 112 and Day 125 due, at least in part, to electron acceptor limitation, as indicated by (1) a decrease in the PAH mass loss rates in the live microcosms, (2) the similarity in the degradation rates in the live and control microcosms after Day 125, and (3) the observed consumption of oxygen and sulfate. PAH degradation in the Sample B microcosms was believed to have also stopped due to oxygen depletion and reduced levels of sulfate sometime between Day 120 and Day 130. However, a greater level of sulfate (11.5 \pm 0.9 mg/L) was present in Sample B relative to Sample A at this

stage of the experiments and sulfate-based biodegradation of some PAH compounds may have continued at a degradation rate similar to the abiotic loss rate.

Net biodegradation rates for each PAH in the live Sample A microcosms and in the live Sample B microcosms (summarized in Table 7) represent composite biodegradation rates under all active electron acceptor conditions. Net degradation rates for fluorene, phenanthrene, and pyrene in the Sample B microcosms (last column of Table 7) represent the average biodegradation rate for each of these compounds under all terminal electron accepting conditions. No biodegradation rates for acenaphthene or benzo(*b*)fluoranthene were calculated, as there was no statistical difference between the live and control Sample B microcosms for these two compounds.

Direct comparison of PAH biodegradation rates from the literature is limited to those studies with comparable laboratory conditions (i.e., static microcosms with native microflora), although not all studies were conducted with a PAH mixture and individual PAH compounds were investigated instead. Durant *et al.* (1995) reported mineralization rates for phenanthrene in five aerobic microcosms varying from 0.73 to 6.94 yr⁻¹ (mean = 3.56 yr⁻¹), compared with 1.13 and 3.28 yr⁻¹ in Samples A and B, respectively. Leduc *et al.* (1992) reported a 100 day half life for fluorene biodegradation under aerobic conditions in a soil slurry reactor. The effective first-order rate (2.5 yr⁻¹) is comparable to the net biodegradation rates for fluorene shown in Table 7 (1.45 and 2.41 yr⁻¹ in Samples A and B, respectively). Juhasz *et al.* (2000) reported soil concentration declines of 19%, 15%, 14%, and 3% after 91 days in static microcosms for fluorene, acenaphthalene, phenanthrene, and pyrene, respectively. Unlike the present study, the soil microcosms in Juhasz *et al.* (2000) were opened twice weekly to facilitate oxygen availability to indigenous PAH degraders. In Sample A of the present study, microbially mediated concentration declines were 30%, 24%, 25%, and 24% at 91 days for fluorene, acenaphthalene, phenanthrene, and pyrene, respectively.

Variability in PAH Degradation with Location

The results from this study reveal differences in the lag period, PAH biodegradability, and the net biodegradation rates between Sample A and Sample B. First, a lag period of approximately 2 months was noted prior to biodegradation in the Sample B live microcosms (Figure 2), whereas no lag period was observed in PAH degradation in the Sample A live microcosms (Figure 1). This variation in lag period between the two locations was possibly due to different contaminant exposure histories of the soil and its impact on the

microbial consortium. McNally *et al.* (1998) observed a lag period prior to the onset of biodegradation when a mixture of anthracene, phenanthrene, and pyrene was introduced as the sole substrate for a pseudomonad strain that had been cultured from an uncontaminated soil. In the same study, PAH biodegradation was observed to begin without a detectable lag period in two separate experiments where the microcosms were inoculated with pseudomonad strains that were cultured from PAH-contaminated soils (McNally *et al.*, 1998). Considering that the Sample A soil sample was collected from a known area of PAH contamination, it was reasonable to assume that the microbial population collected with this soil was acclimated to PAHs, and that the time required for microbial adaptation to PAH degradation was minimal. In contrast, GC-MS analysis of the Sample B soil indicated that exposure of the microbial population in this sample may have been limited to petroleum hydrocarbons that were more volatile and soluble than 3-, 4-, and 5- ring PAHs (Brauner *et al.*, 1999). The time period observed prior to PAH degradation in the Sample B live microcosms of Figure 2 therefore may represent the time required for the microbial population to acclimate to the PAH compounds.

A second difference between the PAH mass loss at the two locations was an observed variation in the biodegradation of PAH compounds. In the Sample A live microcosms, all five PAH compounds were observed to biodegrade, whereas only fluorene, phenanthrene, and pyrene were observed to biodegrade in the live microcosms containing soil from Sample B. The lack of previous exposure to a range of PAHs may explain why biodegradation rates for acenaphthene and benzo(*b*)fluoranthene in Sample B live microcosms were not statistically different from the abiotic rates. In microcosm studies described in Knightes and Peters (1999), acenaphthalene was observed to resist biodegradation in soil samples where other PAHs were biodegraded. Juhasz *et al.* (2000) reported a 12% net mass loss of acenaphthalene after 91 days in noninoculated, periodically aerated soil microcosms but found a 75% net mass loss of acenaphthalene during the same time period in other microcosms containing a mixed bacterial culture inoculant. These observations suggest that while acenaphthalene is less susceptible to biodegradation than other PAHs, mass loss of acenaphthalene may be attributed to biodegradation in the presence of indigenous microbial communities acclimated to acenaphthalene.

A third difference in the study results was in the rate of PAH biodegradation between the two locations. Table 7 presents first-order PAH biodegradation rates for the two samples, indicating that the biodegradation

rates in the live Sample A microcosms were consistently less than the degradation rates observed in the live Sample B microcosms. Biodegradation rates for Sample B microcosms were greater than biodegradation rates found for the Sample A by a factor varying from 1.7 to 2.9 and may be the result of either the presence of excess hydrocarbons, a difference in the amount of catabolically capable biomass, and/or a difference in microbial physiological state. Variation in the physiological state previously has been shown to influence the biodegradation rate of a single substrate in the presence of a compound-specific microbial population poised at different growth levels (Sokol, 1987).

Mass Balance Analysis

Sample A. Based on the first-order degradation rates listed in Table 6, the total PAH mass loss in the Sample A live microcosms was calculated as 0.64 mg. The total observed PAH mass loss in the Sample A live microcosms was calculated by summing the observed losses of each individual PAH. The abiotic portion of this mass loss was calculated as 0.21 mg using the mass loss rates from the control microcosms (Table 6, Column 5). Biodegradation was assumed to be responsible for removing the remaining 0.43 mg, representing roughly 67% of the total hydrocarbon mass loss.

The total theoretical PAH mass loss was estimated using the mass of electron acceptor consumed in the Sample A microcosms and was calculated for both stoichiometric formulations (i.e., with and without growth). PAH mass loss calculations were performed assuming that oxygen and sulfate were the only available electron acceptors, as these electron acceptors were both observed to decline over time in the Sample A live microcosms relative to the Sample A controls. The observed mass of oxygen and sulfate consumed in the Sample A live microcosms was 0.65 mg and 0.27 mg, respectively. Using the stoichiometric relationships for the no-growth model (Table 2), the theoretical mass of PAH loss due to aerobic bio-

degradation in the Sample A live microcosms was calculated as 0.24 mg or 34% of the total hydrocarbon mass loss. Theoretical calculations for sulfate-based PAH mass loss in the Sample A indicated that approximately 0.06 mg (10%) of the PAH mass loss was consumed due to sulfate reduction. As indicated in Table 8, adding the theoretical PAH mass loss under aerobic and sulfate-reducing conditions with the abiotic losses left approximately 23% of the observed mass loss unaccounted for when using the zero yield stoichiometric calculations. Although other microbial processes may have been active in the Sample A live microcosms, there were no indications of iron reduction during the experiment.

Theoretical mass balance calculations were also made for the stoichiometric relationships listed in Table 4, which assumed that a portion of the PAH degraded was converted into biomass. The small yield coefficient for sulfate had a negligible effect on the total PAH predicted to biodegrade. The mass of PAH theoretically biodegraded under aerobic conditions, however, increased to 0.324 mg, or 51% of the total observed PAH loss in the Sample A live microcosms. As indicated in Table 8, inclusion of yield in the theoretical PAH mass loss calculations reduced the difference between the theoretical and observed estimates for PAH mass loss to less than 6% of the total mass loss.

Sample B. Using the procedure described above, the PAH mass loss in the Sample B live microcosms was 0.354 mg. Based on degradation rates observed in the Sample B controls, abiotic mass loss was calculated as 0.054 mg. Biodegradation was assumed to have removed the remaining 0.30 mg of PAH mass, representing roughly 85% of the total PAH mass loss.

The observed mass of oxygen and sulfate consumed in the Sample B live microcosms was 0.65 mg and 0.12 mg, respectively. Using the stoichiometric relationships for the no-growth model (Table 2), the theoretical mass of PAH loss due to aerobic biodegradation in the Sample B microcosms was calculated as

Table 8. Stoichiometric accounting for PAH mass loss in the Sample A live microcosms

Loss Mechanism	No Growth Model		Yield Included	
	PAH mass loss (mg)	% of observed PAH mass loss	PAH mass loss (mg)	% of observed PAH mass loss
Aerobic	0.217	34	0.324	51
Sulfate-reducing	0.063	10	0.063	10
Abiotic	0.210	33	0.210	33
Unaccounted	0.150	23	0.043	6

0.22 mg or 62% of the total hydrocarbon lost. Theoretical calculations for sulfate-based PAH mass loss in the Sample A indicated that approximately 0.023 mg (7%) of the PAH mass loss was consumed due to sulfate reduction. As indicated in Table 9, adding the theoretical PAH mass loss under aerobic and sulfate-reducing conditions with the abiotic losses left approximately 16% of the observed mass loss unaccounted for when using the zero yield stoichiometric calculations. Although other microbial processes may have been active in the Sample B live microcosms, again there were no indications of iron reduction during the experiment.

As with the Sample A microcosms, theoretical mass balance calculations, including biomass growth, were also made for the Sample B microcosms. The small yield coefficient for sulfate had a negligible effect on the total PAH predicted to biodegrade. The mass of PAH theoretically biodegraded under aerobic conditions, however, increased to 0.33 mg, or 93% of the total observed PAH loss in the Sample B live microcosms. As shown in Table 9, the inclusion of yield in the theoretical PAH mass loss calculations for Sample B caused the theoretical PAH mass loss to be overestimated by 15% relative to the observed PAH mass loss. This error may be the result of overestimating the mass of oxygen in the headspace at time zero or other factors not accounted for in the mass balance calculations.

Interpretation of Results. The mass balance analysis using the zero-yield (no growth) approach accounted for 77 to 84% of the total PAH mass loss (biotic and abiotic) compared with 94 to 115% using the modified approach (yield included). Using either approach, agreement between the theoretical and observed PAH mass loss was improved when PAH mass loss under sulfate-reducing conditions was included in mass balance calculations for Sample A. The inclusion of yield in theoretical mass loss calculations for Sample B overestimated (by 15%) the PAH mass loss calculated from observed

changes in concentration. Underprediction by theoretical calculations of observed PAH mass loss may have been caused by incomplete hydrocarbon mineralization, which would reduce the electron acceptor demand per mass of PAH observed to disappear. The accumulation of PAH intermediates was not detected during GC-FID analysis of the CH₂Cl₂-extractable hydrocarbons, implying that PAH oxidation was complete or that the PAH intermediates were irreversibly bound to the soil by oxidative coupling. The overprediction of PAH mass loss for mass balance calculations using the Sample B microcosms with the inclusion of yield may indicate that the estimated theoretical yield is too high for this population.

No distinguishable change in the degradation rate in either of the live microcosms was noted, as would be expected if biodegradation conditions shifted sequentially from aerobic to sulfate reduction. The microcosm vials were not agitated during the experiment, and it is probable that sulfate-reduction may have been active in the portion of the microcosm that was furthest from the headspace, even though oxygen was still detectable in the headspace. Prior to oxygen depletion in the headspace, DO measurements collected just below the water/soil interface were consistently lower (by > 50%) than concentrations measured in the water above the soil (unpublished data).

Conclusions

The results of this study demonstrated that a native microbial consortium could biodegrade a mixture of five PAH compounds under simulated intrinsic conditions, but that oxygen depletion limited complete removal. Three compounds (fluorene, phenanthrene, and pyrene) were observed to biodegrade at two different locations of this site. The two other PAHs (acenaphthene and benzo(*b*)fluoranthene) were observed to biodegrade at sample location A, but mass loss rates in the

Table 9. Stoichiometric accounting for PAH mass loss in the Sample B live microcosms

Loss mechanism	No Growth Model		Yield Included	
	PAH mass loss (mg)	% of observed PAH mass loss	PAH mass loss (mg)	% of observed PAH mass loss
Aerobic	0.220	62	0.330	93
Sulfate-reducing	0.023	7	0.025	7
Abiotic	0.054	15	0.054	15
Unaccounted	0.055	16	<0.055>	<15>

live microcosms from sample B for these compounds were not statistically different than mass loss rates in the control microcosms. In both microcosms sets, PAH degradation rates in the live microcosms became statistically identical to the abiotic degradation rates once oxygen was depleted (at which time, sulfate concentrations were reduced to relatively low levels). The reduction of sulfate to relatively low concentrations in the Sample A and B live microcosms was observed during the periods of biotic PAH mass loss, suggesting the presence of sulfate reducers. As indicated by DO concentration gradients within the vials, portions of the soil were anoxic, which would suggest that sulfate reducers were not subject to oxygen inhibition throughout the vials and would explain simultaneous electron acceptor utilization over time.

Net biodegradation rates compare favorably to aerobic biodegradation rates for fluorene and phenanthrene reported in the literature for similarly designed studies. Our results suggest that for a PAH mixture, there was only a minor variation in rates between the less recalcitrant, 2- and 3-ring PAH compounds and the higher molecular weight 4- and 5-ring PAHs (i.e., pyrene and benzo(*b*)fluoranthene). The data did not indicate sequential degradation of the PAH compounds over time, but that all five PAHs began to degrade in the microcosms at approximately the same point in time. Although abiotic degradation mechanisms were not fully characterized in this study, these results also demonstrated that abiotic PAH mass loss rates may be significant and should be investigated at sites where MNA feasibility is in question. These results also demonstrate the need for microcosm experiments over extended time periods when investigating the biodegradation rates of recalcitrant compounds under intrinsic conditions.

Stoichiometric equations that include biomass yield, developed for PAH oxidation under aerobic and sulfate-reducing conditions, were valuable in assessing the relative contribution of microbially mediated PAH mass loss. Theoretical estimates for the mass of PAH biodegraded in the microcosm sets, based on the mass of electron acceptor consumed, indicate that aerobic biodegradation was the dominant PAH mass loss mechanism in both microcosm sets, while abiotic losses ranged from 15 to 33%, and biotic losses from sulfate-reduction accounted for 7 to 10% of PAH mass loss. Relative to the stoichiometric-based mass balance analysis without biomass yield, the mass balance error decreased when biomass yield was included in the calculations. This result indicated that including PAH conversion to biomass in stoichiometric equations of PAH oxidation may improve estimates of PAH mass loss based on the mass of electron acceptor utilized,

although further research is needed to determine whether this approach will consistently reduce the discrepancy between observed and theoretical mass estimates.

The results of this study provided one line of evidence that MNA is a potential remediation option for PAH contamination at this site. However, the results suggest that a nonuniform pattern of biodegradation may be expected and that the recalcitrance of acenaphthene and benzo(*b*)fluoranthene should be considered. With the presence of active PAH degraders at this site, demonstrated through the results of the microcosm study, bioventing pilot tests were performed and a full-scale system was implemented with MNA.

Acknowledgments

Partial funding for this research was received from the Via Foundation of the Charles E. Via, Jr. Department of Civil and Environmental Engineering at Virginia Polytechnic Institute and State University. Dr. Wen Lee, Law Engineering and Environmental Services (Sterling, Virginia office) provided advice and expertise at the field site. The authors thank Marilyn Grender and Julie Petruska for their assistance and advice during the experimental portion of this work.

References

- American Public Health Association, American Water Works Association, and Water Environment Federation. 1998. *Standard Methods for the Examination of Water and Wastewater*, 20th ed., Washington, DC.
- Bauer, J.E. and D.G. Capone. 1988. Effects of Co-occurring Aromatic Hydrocarbons on Degradation of Individual Polycyclic Aromatic Hydrocarbons in Marine Sediment Slurries. *Appl. Environ. Microbiol.*, 54(7):1649-1655.
- Brauner, J.S., M.A. Widdowson, J.T. Novak, and N.G. Love. 1999. Intrinsic Bioremediation of PAH Compounds at a Fuel-Contaminated Site In: A. Leeson and B.C. Alleman (Eds.), *Bioremediation Technologies for Polycyclic Aromatic Hydrocarbons*. 5(8):19-24. Battelle Press: Columbus, OH.
- Brown, D.G., C.D. Knightes, and C.A. Peters. 1999. Risk Assessment of Polycyclic Aromatic Hydrocarbon NAPLs using Component Fractions. *Environ. Sci. Tech.* 33(24):4357-4363.
- Coates, J.D., R.T. Anderson, and D.R. Lovley. 1996. Oxidation of Polycyclic Aromatic Hydrocarbons under Sulfate-Reducing Conditions. *Appl. Environ. Microbiol.* 62(3):1099-1101.
- Coates, J.D., J. Woodward, J. Allen, P. Philp, and D.R. Lovley. 1997. Anaerobic Degradation of Polycyclic Aromatic Hydrocarbons and Alkanes in Petroleum-Contaminated Marine Harbor Sediments. *Appl. Environ. Microbiol.* 63(9):3589-3593.

- Durant, N.D., L.P. Wilson, and E.J. Bouwer. 1995. Microcosm Studies of Subsurface PAH-Degrading Bacteria from a Former Manufactured Gas Plant. *J. Contam. Hydrol.* 17:213-237.
- Gibson, D.T., V. Mahadevan, D.M. Jerina, H.J. Hagi, and H.J.C. Yeh. 1975. Oxidation of the Carcinogens Benzo(a)Pyrene and Benzo(a)Anthracene to Dihydrodiols by a Bacterium. *Science* 189:295-297.
- Grady, C.P.L., G.T. Daigger, and H.C. Lim. 1999. *Biological Wastewater Treatment, 2nd ed.*, pp. 61-78. Marcel Dekker, Inc., New York.
- Hatzinger, P.B. and M. Alexander. 1995. Effect of Aging of Chemicals in Soil on their Biodegradability and Extractability. *Environ. Sci. Technol.* 29(2):537-545.
- Juhasz, A.L., G.A. Stanley, and M.L. Brtiz. 2000. Degradation of High Molecular Weight PAHs in Contaminated Soil by a Bacterial Consortium: Effects of Microtox and Mutagenicity Bioassays. *Biorem. J.* 4(4):271-283.
- Karickhoff, S.W. 1980. Sorption Kinetics of Hydrophobic Pollutants in Natural Sediments. In: R.A. Baker (Ed.), *Contaminants and Sediments. Volume 2: Fate and Transport Studies, Modeling, Toxicity*, pp. 193-205. Ann Arbor Science, Ann Arbor, MI.
- Knightes, C.D. and C.A. Peters. 1999. Measurement and Comparison of Monod Biodegradation Parameters of PAHs. In: A. Leeson and B.C. Alleman (Eds.), *Bioremediation Technologies for Polycyclic Aromatic Hydrocarbons*. 5(8):173-178. Battelle Press, Columbus, OH.
- Leduc, R., R. Sampson, B. Al-Bashir, J. Al-Hawari, and T. Cseh. 1992. Biotic and Abiotic Disappearance of Four PAH Compounds from Flooded Soil under Various Redox Conditions. *Water Sci. Tech.* 26(1-2):51-60.
- McCarty, P.L. 1971. *Energetics and Bacterial Growth. Organic Compounds in Aquatic Environments*, Marcel Dekker, Inc., New York.
- McFarland, M.J. and R.C. Sims. 1991. Thermodynamic Framework for Evaluating PAH Degradation in the Subsurface. *Ground Water* 29(9):885-896.
- McNally, D.L., J.R. Mihelcic, and D.R. Lueking. 1998. Biodegradation of Three- and Four-ring Polycyclic Aromatic Hydrocarbons under Aerobic and Denitrifying Conditions. *Environ. Sci. Technol.* 32(17):2633-2639.
- Mihelcic, J.R. and R.G. Luthy. 1988a. Degradation of Polycyclic Aromatic Hydrocarbon Compounds under Various Redox Conditions in Soil-Water Systems." *Appl. Environ. Microbiol.* 54(5):1182-1187.
- Mihelcic, J.R. and R.G. Luthy. 1988b. Microbial Degradation of Acenaphthene and Naphthalene under Denitrification Conditions in Soil-Water Systems. *Appl. Environ. Microbiol.* 54(5):1188-1198.
- National Research Council. 2000. *Natural Attenuation for Groundwater Remediation*. National Academy Press, Washington, D.C.
- Novak, J.T., W.B. Burgos, and A. Bhandari. 1998. Reversible and Irreversible Binding of Organics to Soils and the Effect of Biodegradation. In: H. Rubin, N. Narkis, and J. Carberry (Eds.) *Soil and Aquifer Pollution. Non-aqueous Phase Liquids – Contamination and Reclamation*. Pp. 191-206. Springer-Verlag, New York.
- Ott, R.L. 1992. *An Introduction to Statistical Methods and Data Analysis, 4th ed.*. Duxbury Press, Belmont, CA. pp.716-721.
- Peters, C.A., C.D. Knightes, and D.G. Brown. 1999. Long-term Composition Dynamics of PAH-Containing NAPLs and Implications for Risk Assessment. *Environ. Sci. Technol.* 33(24):4499-4507.
- Sokol, W. 1987. Oxidation of an Inhibitory Substrate by Washed Cells (Oxidation of Phenol by *Psuedomonas putida*). *Biotech. Bioeng.* 30(8):921-927.
- Stumm, W. and J.J. Morgan. 1995. *Aquatic Chemistry, 3rd ed.*, Chap. 7. J. Wiley & Sons, New York.
- U.S. EPA. 1999. *Use of Monitored Natural Attenuation at Superfund, RCRA Corrective Action, and Underground Storage Tank Sites*. OSWER Directive 9200.4-17P.
- Wilson, B.H., J.T. Wilson, and D. Luce. 1996. Data and Interpretation of Microcosm Studies for Chlorinated Compounds. In: *Proceedings of the Symposium on Natural Attenuation of Chlorinated Organics in Ground Water*. pp. 23-30. Dallas, TX.
- Zehnder, A.J.B. and W. Stumm. 1988. Geochemistry and Biogeochemistry of Anaerobic Habitats. In: A.J.B. Zehnder (Ed.), *Biology of Anaerobic Microorganisms*, pp. 1-38. J. Wiley and Sons, New York.